Краткие сообщения ОИЯИ № 2[48]-91 *JINR Rapid Communications No.2[48]-91*
УДК 539.1.072

ELECTRICAL TRANSPARENCY OF GRIDS USED IN GASEOUS PARTICLE DETECTORS

D.M.Khazins, A.A.Kuritchin

Electrical transparency of wire grids used in gaseous particle detectors is examined. A method for measuring the transparency is developed. The experimental results are presented for two kinds of grids (linear grids made from parallel wires and meshes made from crossed wires) with various radius-to-pitch ratios. The experimental results are compared with the transparency calculations.

The investigation has been performed at the Laboratory of Nuclear Problems, JINR.

Электрическая прозрачность сеток, применяемых в газоразрядных детекторах частиц

Д.М.Хазинс, А.А.Курицин

Исследуется электрическая прозрачность проволочных сеток, используемых в газоразрядных детекторах частиц. Разработан метод измерения прозрачности. Представлены результаты измерений для двух типов сеток (линейных сеток из параллельных проволок и клетчатых сеток, изготовленных из скрещенных проволок) для различных отношений радиус-шаг. Экспериментальные результаты сравниваются с результатами аналитических вычислений.

Работа выполнена в Лаборатории ядерных проблем ОИЯИ.

Introduction

Wire grids are widely used in gaseous detectors of elementary particles such as time-projection chamber, X-ray detectors, multistep chambers, etc., to separate the drift or conversion gaps from the registering ones.

The grids usually must satisfy two contradictory requirements. On the one hand the grids must have maximal electrical transparency or, in other words, let the maximal number of drifting electrons pass through itself. From this point of view sparse grids with thin wires are good enough. On the other hand the nonuniformity of the electri-

cal field created by the grid must be as small as possible. That naturally calls for dense grids with closely situated wires. So the detailed knowledge about geometrical parameters of grids on its characteristics (transparency and field nonuniformity) are needed.

In this work the results of a study of electrical transparency of various grids as a function of their geometrical parameters and surrounding electrical fields are presented for both linear grids made from parallel and equidistantly placed wires and meshes made from crossed wires. Particular attention is paid to dense grids and meshes.

The transparency of sparse grids (with small ratio of the wire radius (R) to the wire pitch (S)) can be analytically calculated [1]. Here we mean the grids placed in gaseous environment. In this case electrons and ions are drifting along with electrical field lines contrary to the vacuum case. The results of these calculations (see also the Appendix) may be represented as follows.

In Fig.1 four configurations of electrical field versus various values of the parameter

$$X = \frac{Q}{R|E_0|} e,$$

are shown. Here Q is the linear density of the wire charge, E_0 is the value of the electrical field intensity created by outer electrodes (the cathode and anode) in the wire position, R is the wire radius, $e = \pm 1$ corresponding to the sign of drifting charges.

To make it more definite let us consider the electrical transparency (η) of the grid (Fig.1) for positive ions.

If $x > 1$, all the field lines start from the anode and pass through the grid. This means that the ions pass through the grid too and transparency is

$$\eta = 1. \qquad (1)$$

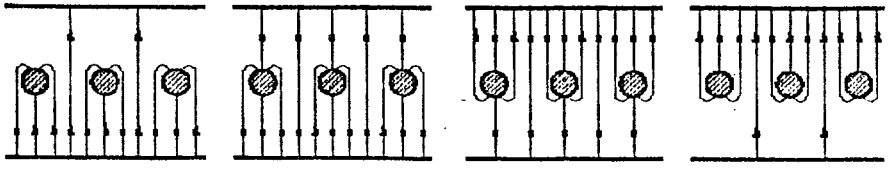

Fig.1. Field configurations in the chamber gaps versus the X-parameter.

If $x < -1$, transparency is proportional to the number of field lines collected by the cathode. If the cathode and anode gaps are big enough, so that the intensity of electric fields near them may be considered uniform (E_c and E_a), then transparency is

$$\eta = \frac{E_a}{E_c}. \qquad (2)$$

The situation is more complicated for $|x| < 1$. It is necessary to use the following equation (see the Appendix)

$$\eta = \frac{1 - 4\frac{R}{S}\left(\sqrt{1 - x^2} + x \arcsin x\right)}{1 - 2\pi\frac{R}{S}x}. \qquad (3)$$

The formulae (1)÷(3) are correct for sparse linear grids with ratio $R/S \leq 0.075$, which has been checked by experiment [1,2]. To find out the correctness limit of the calculations and the transparency of dense linear grids and meshes we performed some measurements with a special model.

Experimental Method

Our model (Fig.2) consists of an anode (1), a cathode (2) and a grid (3) assembled together by plexiglas spacers (4). The working surface of each electrode is 120x120 mm^2. The cathode-grid gap (L_c) was chosen (see below) equal to 20.7 mm, the grid-anode gap (L_a) varied from 4.8 mm to 6.7 mm. The changeable grid was made from copper wires with diameters from 0.025 to 0.325 mm and had the pitch size 3 mm.

As a source of charged particles, a corona discharge on the cathode was chosen. With this aim the holes 6 mm in diameter with 10 mm pitch in both directions (a total of 121 holes) were made in the cathode surface. In the center of each hole the needles were set with tips sticking out about 0.5 mm above the cathode surface. When the high voltage ($U_c = -2.6 \div -3.0$ kV) is applied to the needles, the corona discharge is set between the needle tips and the grounded cathode surface. If there is some voltage on the anode and the grid, a part of ions leave the corona region and drift to the anode. One can then determine the grid electrical transparency by measuring the anode (I_a) and the grid (I_a) currents by the formula:

$$\eta = \frac{I_a}{I_a + I_g}. \qquad (4)$$

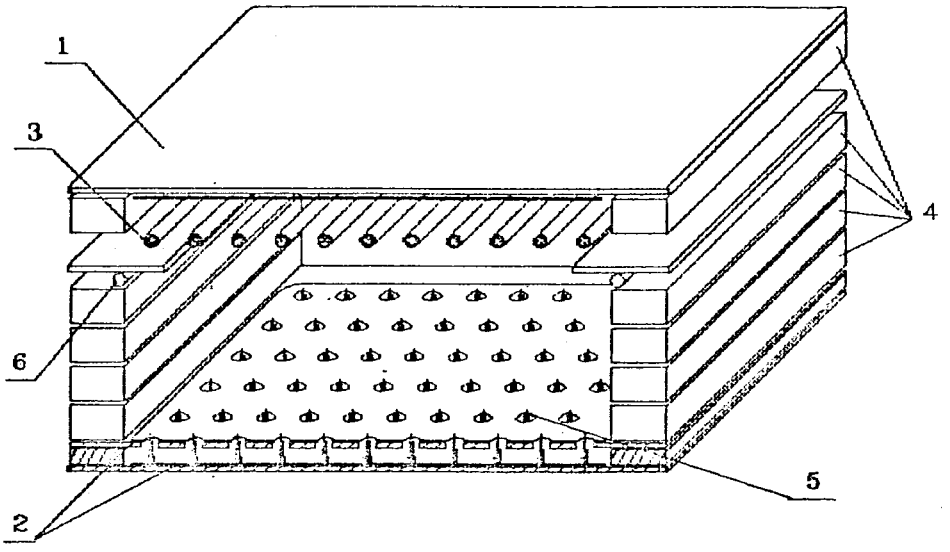

Fig.2. Design of the experimental model: (1) anode, (2) cathode, (3) grid, (4) spacers, (5) needles, (6) guard wire.

The characteristic value of the corona current was $I_{corona} \simeq 120\ \mu A$. And the summary current in the cathode-grid gap ($I_a + I_g$) varied from 2 to 12 μA depending on the electrode potentials.

To avoid the surface currents from the cathode to the grid a guard wire (6) was set under the grid.

For decreasing of edge effects the mylar sheet with the inner window 100x100 mm in size was set in the cathode-grip gap 5 mm below the grid. The difference between the transparency values measured with and without that sheet was smaller than 4%.

As is said above, we used the cathode of special shape. This leads to a strong nonuniformity of the electrical field near the cathode surface. The influence of the nonuniformity on the transparency determination may be decreased by enlarging the cathode-grid gap. The measurements for various distances L_c showed that starting from L_c = = 19 mm the value of transparency is not changed and in the further measurements we used L_c = 20.7 mm.

The influence of the anode-grid distance on transparency was not noticed. All the measurements were done with three values L_a = 4.8, 5.8 and 6.7 mm and showed practically the same results.

This model does not have an air-proof casing and air was used as a working gas. The open construction allows free access to the elec-

trodes and easy changing of their configuration. However, the use of air as a working gas means that the electric charge is carried by slowly moving negative oxygen ions (due to electrons attached to oxygen molecules). Consequently a large volume charge appears, which considerably changes the electric fields in the gaps. In the data analyses this change has been taken into account.

Experimental Results

The degree of accuracy with which our model allows the measurement of the transparency (after corrections) can be estimated from Figs. 3 and 4, where the results of measurements with sparse linear grids are shown with the results of calculations according to formulae (1)÷(3). The standard deviation of the experimental points from the curves is 1.8 %. In Fig.3 the data without correction for the volume charge effect are also shown. Disagreement in this case is 20 %.

In Figs.5-7 the results of transparency measurements for dense linear grids are shown. The systematic deviation from the calculations becomes noticeable as the ratio R/S increases, and for R/S = 0.05 the calculations are in complete disagreement with the measurements. It should be noted that the measured values of transparency in all cases are above the calculated ones.

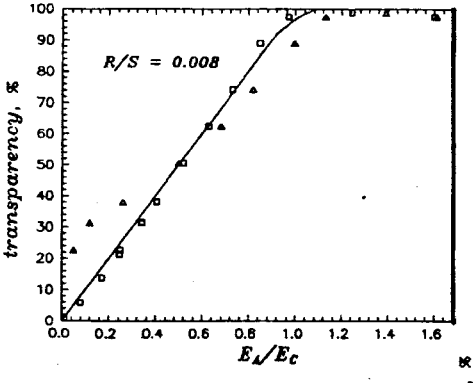

Fig.3. Transparency for the linear grid with R = 0.025 mm and S = 3 mm, Δ — points without corrections for the volume charge influence, □ — points with corrections for the volume charge influence, —— — curve calculated by formulae (1)÷(3).

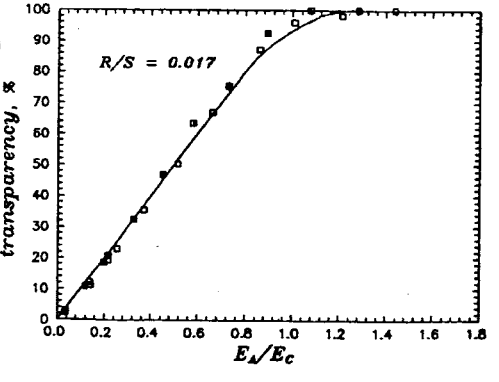

Fig.4. The same as in Fig.3 for the grid with R = 0.050 mm and S = 3 mm.

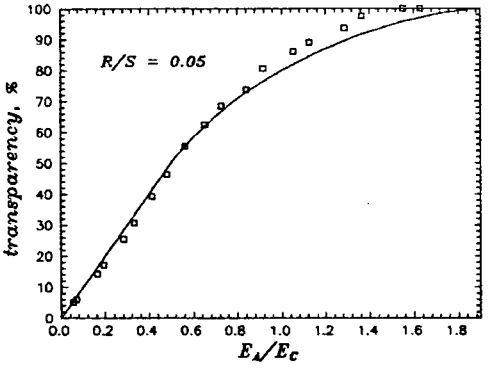

Fig.5. The same as in Fig.3 for the grid with R = 0.150 mm and S = 3 mm.

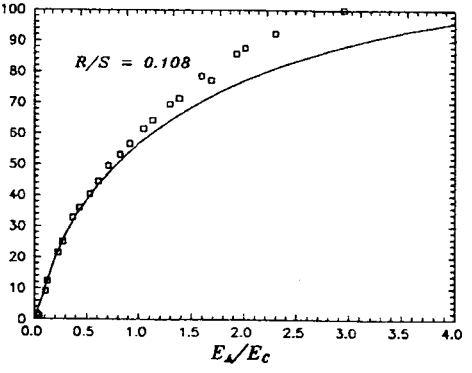

Fig.6. The same as in Fig.3 for the grid with R = 0.325 mm and S = 3 mm.

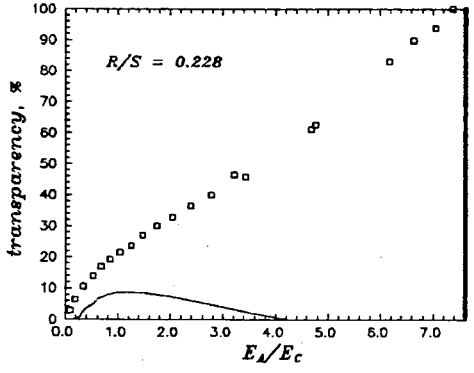

Fig.7. The same as in Fig.3 for the grid with R = 0.685 mm and S = 3 mm.

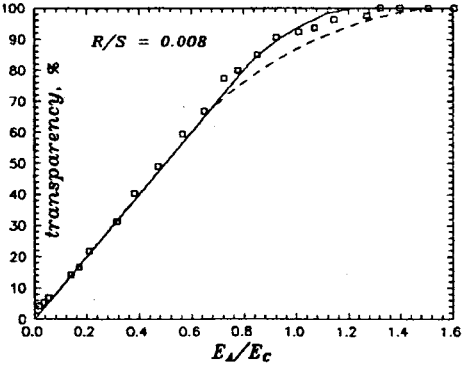

Fig.8. The same as in Fig.3 for the mesh with R = 0.050 mm and S = 3 mm. Dashed is curve calculated by formulae (1)÷(3) for R/S twice as big as the real ratio.

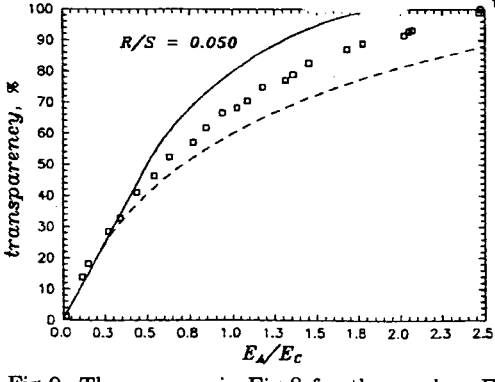

Fig.9. The same as in Fig.8 for the mesh with R = 0.150 mm and S = 3 mm.

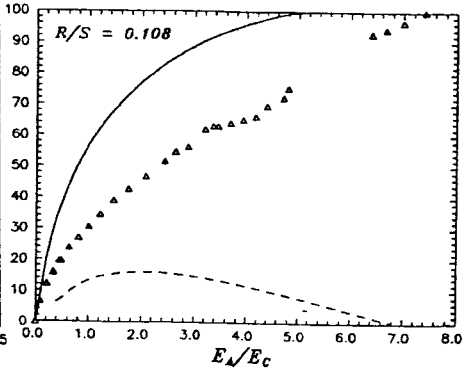

Fig.10. The same as in Fig.8 for the mesh with R = 0.325 mm and S = 3 mm.

In Figs.8-10 we show the results for the meshes of different density. There are no theoretical estimations for these grids. Nevertheless, we also present the transparency curves obtained with formulae (1)÷(3) for two values of the S-parameter: one is equal to the wire pitch (as if the transverse wires are removed), and the other is equal to half of the wire pitch (as if the transverse wires are rotated by 90° and placed between the longitudinal ones). All the measured points lie between these two curves, so formulae (1)÷(3) can be used for rough estimation of the mesh transparency for R/S up to 0.228. The data in all figures are shown as functions of the ratio of the field intensities near the anode and the cathode.

In order to connect them with voltage of the grid-anode gap (U_a) and of the grid-cathode gap (U_c) it is convenient to write the potential created by the grid with the average charge density σ at a sufficiently large distance from it L > S as

$$F = 2\pi\sigma(L + \delta), \tag{5}$$

where the parameter δ depends only on the geometry of the grid.

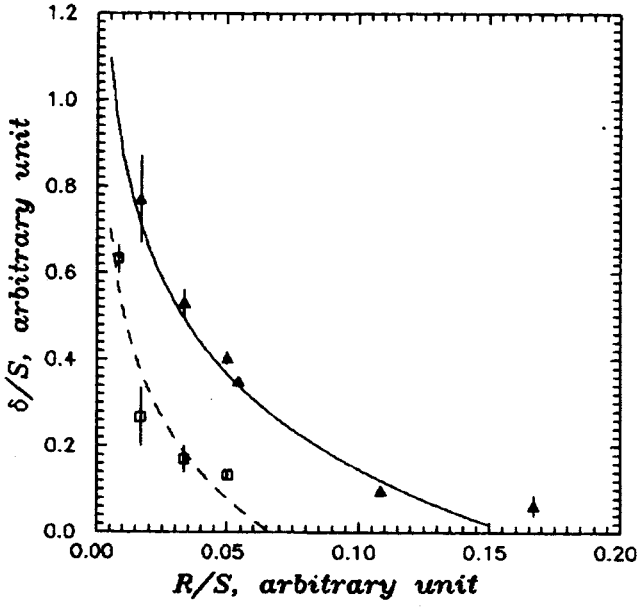

Fig.11. Dependence of δ/S on R/S, Δ — measured values δ/s for the linear grids, □ — measured values δ/S for the meshes, —— — curve calculated by formula (7), --- — curve calculated by formula (7) for R/S twice as big as the real ratio.

With this form of the grid potential one can obtain the electrical field intensity in the grid-anode gap

$$E_a = \frac{U_a}{L_a}\left[1 - \delta \frac{1 + \frac{U_a L_c}{U_c L_a}}{2L_a + \delta(1 + \frac{L_a}{L_c})}\right]. \qquad (6)$$

The formula for E_c can be obtained by exchanging the indices a and c.

The parameter δ for sparse linear grids can be calculated

$$\delta = -\frac{S}{\pi} \ln\left(2\mathrm{sh}\left(\frac{\pi R}{S}\right)\right). \qquad (7)$$

For other grids δ can be found by measuring the electrical capacitance of the grid relatively to the flat electrodes. Some results of these measurements compared with the calculations by formula (7) are presented in Fig.11.

Conclusions

We believe that the experimental results presented in Figs.3 ÷10 will be useful for estimation of electrical transparency of the grids used in particle detectors.

The calculations based on formulae (1) ÷(3) are well appropriate for linear grids with $R/S \leq 0.05$ and may be used as a rather close lower limit of the transparency up to $R/S \simeq 0.1$.

The transparency for the meshes with $R/S < 0.05$ can also be estimated with formulae (1) ÷(3) which gives an upper limit of the transparency if the real value S is used, or a lower limit if the half of the real wire pitch is used as parameter S.

The electrical transparency of even very dense linear grids and meshes (with the optical transparency $\simeq 0.5$) reaches 100 % at the sufficiently high anode-to-cathode electrical field intensity ratio (Figs.7 and 10).

Appendix

Here we present the derivation of formula (3) by a method somewhat different from (1).

To begin with, let us consider the problem of charge density distribution $q(\phi)$ on the surface of a single wire with radius R in an external

electrical field E_0 orthogonal to the wire axis. The polar angle ϕ is defined relatively to the field direction. From the condition $E_{tang.} = 0$ the equation follows:

$$\int_0^{2\pi} q(\psi)\, \mathrm{ctg}\, \frac{\psi - \phi}{2}\, d\phi + E_0 \cos\phi = 0. \tag{A1}$$

The solution has the form:

$$q(\phi) = \frac{E_0}{2\pi} \sin\phi + \frac{Q}{2\pi R}, \tag{A2}$$

where $Q = \int_0^{2\pi} q(\phi) \cdot d\phi$ is the linear charge density on the wire.

Hence the electric field intensity on the wire surface is:

$$E = \frac{2 \cdot Q}{R} + 2E_0 \cdot \sin\phi. \tag{A3}$$

For $|Q| < |RE_0|$ and for the angle range $\phi_1 < \phi < 2\pi - \phi_1$, where $\phi_1 = \arcsin[-\frac{Q}{RE_0}]$, the field lines enter the wire surface and the positive charges drifting along them are captured by the wire. The electric field flux captured by a unit of wire length is:

$$F_1 = -\int_{\phi_1}^{2\pi-\phi_1} ER\, d\phi = 4\sqrt{E_0^2R^2 - Q^2} + 4Q \arcsin\frac{Q}{E_0 R} - 2\pi Q. \tag{A4}$$

Now let us consider a linear grid with wire pitch S. For large distances from the grid (comparable with S) the electric field flux from the anode to the grid corresponding to one wire of unit length is:

$$F = [E_0 - 2\pi\frac{Q}{S}]S. \tag{A5}$$

If the grid is sufficiently sparse so that the field on the wire surface induced by neighboring wires can be neglected the formula (A4) is correct. Then the electric transparency is:

$$\eta = 1 - \frac{F_1}{F} = \frac{E_0 S - 4(\sqrt{E_0^2R^2 - Q^2} + Q\arcsin\frac{Q}{E_0 R}}{E_0 S - 2\pi Q}. \tag{A6}$$

This formula can be generalized for negative particles coming from the cathode by introducing $X = \frac{Qe}{R|E_0|}$, where $e = \pm 1$ depending on the sign of the drifting particles. Finally, for grid transparency we obtain:

$$\eta = \frac{1 - 4\frac{R}{S}(\sqrt{1 - x^2} + x \arcsin x)}{1 - 2\pi\frac{R}{S}x}. \qquad (A7)$$

References

1. Bunemann O. et al. — Can. J. Res., 1949 No.1, A27.
2. Nemethy P. et al. — NIM, 1983, 212, p.273.

Received on April 10, 1991.